Research Square

Preprints are preliminary reports that have not undergone peer review.
They should not be considered conclusive, used to inform clinical practice,
or referenced by the media as validated information.

Effect of Cutting Edge Preparation by Abrasive Brushing on End Mill Wear and Surface Quality of Aisi P20 Steel

Wiliam Buckell

Luccas Augusto Pedrassani Delgado

lapdelgado@ucs.br

University of Caxias do Sul: Universidade de Caxias do Sul https://orcid.org/0009-0000-4610-6589

Rodrigo Panosso Zeilmann

UCS: Universidade de Caxias do Sul

Research Article

Keywords: Edge treatment, Microgeometry, Tool performance, Roughness, Mold steel

Posted Date: July 27th, 2026

DOI: https://doi.org/10.21203/rs.3.rs-10426454/v1

License: This work is licensed under a Creative Commons Attribution 4.0 International License.
Read Full License

EFFECT OF CUTTING EDGE PREPARATION BY ABRASIVE BRUSHING ON END MILL WEAR AND SURFACE QUALITY OF AISI P20 STEEL

Wiliam Buckell[1], Luccas Augusto Pedrassani Delgado[1]*, Rodrigo Panosso Zeilmann[1]

[1] University of Caxias do Sul (UCS), Francisco Getúlio Vargas 1130, Brazil.

*Corresponding Author: **lapdelgado@ucs.br**

Orcid: 0009-0000-4610-6589; 0000-0001-7753-3049

Abstract

The brushing process is widely used in the industry for cutting edge preparation due to its effectiveness across various tool types, low implementation costs, and short operation times. Proper edge microgeometry removes manufacturing defects, enhancing the mechanical stability and tool life of cutting wedges. This study investigates the cutting edge preparation of carbide end mills using a pneumatic brushing process, analyzing the direct impacts of process parameters on edge microgeometry, tool wear, and workpiece surface quality. Preliminary tests on linear cutting edges were performed to determine the optimal parameters before preparing helical end mills. Silicon carbide (SiC) and aluminum oxide (Al_2O_3) micro-abrasives were utilized to alter the radius and shape of the cutting edge. Brushing parameters (angle, contact depth, and rotational speed) were evaluated via contact techniques and scanning electron microscopy (SEM). Milling tests were then conducted on AISI P20 steel to compare treated and untreated tools. Brushing parameters directly dictated the edge microgeometry. The brush angle influenced the rounding shape, contact depth significantly impacted rounding size and shape, and higher rotational speeds increased the material removal rate. While some parameter sets induced minor edge irregularities, the SiC micro-abrasive generated satisfactory, defect-free geometries in most combinations, with "Configuration 15" yielding the most suitable rounding. In machining tests, the brushed tool effectively controlled wear mechanisms, demonstrating a 21% increase in tool life when a flank wear of 0.2 mm was reached. Furthermore, the brushing condition reduced Ra and Rz roughness at both the beginning and end of the tool life, although the untreated tool obtained lower Rz1max values, as corroborated by optical texture analysis. The abrasive brushing process using SiC sheets is an efficient, cost-effective method for engineering precise cutting edge microgeometries that significantly enhance tool life and control surface quality during milling.

Keywords: Edge treatment; Microgeometry; Tool performance; Roughness; Mold steel

1. Introduction

In the manufacturing area, the machining process plays an important role in the production of a wide variety of parts. As time progresses, the criteria for tolerances and requirements become more rigorous, with the objective of meeting the standards in the machining production. At the same time, the industry pursues two main objectives. The first one, is to increase productivity and the quality of the generated product. The second, is a reduction in process time and

manufacturing costs. Thus, the search for improvements becomes necessary (Toenshoff and Denkena, 2013; Wegener et al 2016).

The cutting tool is a key part of the manufacturing process. The cutting edge's shape and condition are crucial for the machining process as they affect the mechanical and thermal stresses in the cutting region. (Denkena; Biermann, 2014). After grinding, the cutting edge can have burrs, irregularities, micro-chipping and other defects. This affects the cutting edge's mechanical strength, tool performance and workpiece surface quality. (Tikal, 2009; Denkena et al., 2013).

A process known as cutting edge preparation was developed to mitigate this effect. The fundamental objective of this process is to reduce defects originating from the manufacturing process. This is achieved as a result of removing material from the cutting edge, to achieve a uniform transition surface between the rake face and flank face. The benefits are an increase in the stability of the cutting edge, reduced thermal and mechanical stresses. These factors result in an enhancement in the tool life and reliability of the cutting process (Denkena et al., 2011; Zhuang et al., 2021; Denkena et al., 2005).

The brushing process is characterized by its non-defined geometry, in contrast to other edge preparation processes. Material removal is achieved through abrasion. Filaments of nylon, SiC or Al_2O_3 are commonly employed in the process of brushing (Stango, 2002; Overholser 2003; Rodríguez 2009). The process parameters directly influence the cutting edge. An increase in brush rotation speed leads to higher mechanical and thermal stresses on the filament, causing flaking and loosening of the abrasive grains. Wear of the filaments is important for material removal. Shortening of the filaments and wear of the abrasive grains over time reduces the rate of material removal, increasing the process time. This leads to a decrease in the K factor shape values (Denkena et al., 2009; Bergs et al., 2020).

In a study conducted by Breidenstein et al. (Breidenstein et al., 2024), the impact of edge preparation by brushing and grinding processes on the residual stress of PCD and PcBN inserts was investigated. The results show that the brushing process induced less compressive residual stress, as the material is removed from the surface of the tool, exposing the substrate that was not affected by the manufacturing process. Process parameters also influenced the residual stress present on both substrates.

Frank and Otto (Frank and Otto, 2019) carried out a precision brushing preparation in micro end mills to machine a DIN X37CrMoV5–1 workpiece. The brushing process was capable to improve the size of the edge radius r_β from 4 µm to 10 µm. In the machining tests, the prepared tool experienced a 33% reduction in the flank wear to VB = 70 µm and enhanced its mechanical strength against micro chipping. Moreover, the brushed tool exhibits a reduction in the edge roughness.

Rodríguez (Rodríguez, 2009) in its study compared the brushing process with nylon abrasive and the brushing-polishing with the abrasive jet machining. The surface finishing of the brushing-polishing process showed a greater refinement than the other preparation methods.

All the preparation processes were able to increase the tool life of the end mill, and when comparing the processes with the same cutting edge radius of 12 μm, the brushed-polished tool outperformed the other conditions.

Zeilmann et al. (2018) utilized the nylon filament with SiC micro-abrasive brush and drag finish with H 4/400 media for cutting edge preparation of carbide mills. Both preparation methods improved the edge surface quality. In the primary edge, the brushing condition resulted in the highest roughness, as in the secondary edge, the drag finish process had the lowest values. Both edge preparation methods decreased roughness of the workpiece surface under dry conditions.

Bouzakis et al. (Bouzakis et al., 2014) prepared carbide inserts using several processes, including brushing, and worked with four different materials. The objective was to verify the impact on tool life, cutting temperatures, and coating properties. Edge preparation improved coating adhesion to the substrate. Residual stress decreased with the edge radius due to greater material removal. For tool life, brushing decreased when machining stainless steel 304L and Ti6Al4V, but increased the tool life of 42CrMo4+QT by 26%. This process also increased the cutting length of Inconel 718 by 30%.

As indicated previously, the preparation of the cutting edge and its parameters have a significant impact on the resultant microgeometry. Therefore, the aim of this study is to verify the influence of edge preparation by means of brushing. Abrasive nylon filaments with two different micro-abrasives were employed to treat the microgeometry of carbide end mills that machined AISI P20 steel. Through brushing tests on a prototype end mill tool, it was possible to understand the impact of different configurations of brushing parameters and micro-abrasive in the microgeometry of the cutting edge. The main objective was to find the best configuration to effectively treat the end mill used in the machining tests, and compare the tool performance and surface quality of the workpiece with an unprepared end mill.

2. Materials and Methods

To understand the influence of parameters on the brushing process, a specific methodology was developed. The experiments were divided into two stages: brushing tests using various parameters on prototype end mills to evaluate cutting-edge conditions, and machining tests applying the optimal parameter combination directly to carbide end mills.

2.1 Experimental Conditions

Experimental tests were conducted in the Hartford LG-500 CNC machine with 15 kW of power, 5.5 kW spindle power and maximum rotation speed of 10,000 rev/min. For the experiment, the workpiece material used was the AISI P20 steel, primarily utilized in die cast and molds. The measured chemical composition can be seen in Table 1. It was tempered and quenched, which resulted in 37 ± 1 HRC hardness. The dimensions were 252 mm length, 80 mm wide and 60 mm height.

Table 1. Chemical composition of AISI P20 steel.

Element	C	Si	Mn	P	S	Cr	Mo	Ni	Co	Cu	Fe
Content (%)	0.41	0.38	1.46	0.02	0.38	2.03	0.20	0.72	0.11	0.12	As balance

Cutting parameters were maintained constant during the machining tests, cutting speed (v_c) was 180 m/min, feed (f_z) was set 0.05 mm/tooth and axial (a_p) and radial (a_e) depth was 0.5 mm and 0.2 mm respectively. The experimental parameters were selected based on preliminary testing The machining strategy was using down milling and no cutting fluid.

The end mills employed in the machining tests are manufactured by Secta Tools. They have a nominal diameter of 6 mm, 4 cutting edges, uncoated and the substrate is cemented carbide K40 grade with submicron grain size. The wedge angle β is 72°, clearance angle α is 10°, rake angle γ is 8° and the helix angle is 30°. The total length of the end mill is 80.5 mm, with an effective cutting area of 31 mm.

For the test, the end of tool life criterion was adopted based on flank wear VB_{MAX} = 0.2 mm or chipping surpassing the same dimension. Simultaneously, an end of test criterion was employed, limiting the test to 30 linear meters. Every 5.04 meters machined, the tool was inspected to measure the wear on the cutting edges, which correspond to 20 passes of the tool along the length of the workpiece.

In the brushing test, each preparation was qualitatively evaluated using a Tescan Mira 3 scanning electron microscope (SEM) to verify the microgeometry and surface quality directly on the cutting edge. Also, it was used to identify the wear types and mechanisms.

The profile of the cutting edge was assessed using a contact technique with a Mahr contour measuring station, model MarSurf CD 280, moving the tip at 0.20 mm/s over measuring length of 2 mm, collecting 2000 position points to generate the profile. To better characterize the size and the shape, was employed the method proposed by Denkena et al. (Denkena et al., 2002) called K form-factor, which consists of five parameters for a detailed description of the cutting edge.

To evaluate the roughness of the workpiece, the parameters Ra, Rz, and Rz1max (ISO 4287) were employed. Texture images were taken at the same measurement location for the beginning and for the region where the tool reached the end of its life. The roughness values were obtained using a Mitutoyo SJ-301 portable roughness tester with a resolution of 0.01 μm, a diamond probe tip radius of 5 μm, and a coincidence angle of 90°. The textures were obtained by images using the Entex TNE-10B universal measurement trinocular stereoscope.

2.2 Brushing Configuration Tests

In these tests, the main objective was to ascertain the impact of the parameters in the brushing process on the size and quality of the cutting edge. To this end, a prototype end mill was developed to allow for the execution of brushing tests. Three end mills with a diameter of 8 mm were fabricated, exhibiting notable similarities to the main end mill in terms of wedge configuration and utilization of the same WC substrate. However, the biggest difference in the macrogeometry correspond to a helix angle $\lambda = 0°$ and only two cutting edges. The prototype mill is shown in Figure 1, along with macrogeometry characteristics and information about the brushing process setup.

Figure 1. Abrasive brushing setup for the prototype mill

To facilitate the implementation of brushing operations, the tool has been subdivided into different areas, as indicated by green markings on the cutting edge. Each area corresponds to a distinct brushing configuration. This strategy enables the execution of eight tests per tool, i.e. four tests per cutting edge. The brushing process was performed through the utilization of the axial movement of the machine center spindle, where the tool was fixed. The abrasive disc was subjected to alternating upward and downward movements, which resulted in a traverse motion of 7.5 mm at a feed rate of 120 mm/min. The disc traversed 16 times over a duration of 60 seconds. The radial depth of the disc was $a_{eb} = 1.5$ mm.

The brushing process utilized Scotch-Brite™ production clean and finish sheets from 3M as the abrasive. These sheets consist of a non-woven nylon web that is embedded with micro-abrasives using a waterproof resin. Two types of abrasives were used: the first was composed aluminum oxide (Al_2O_3) with 320 grit, classified as very fine, and the second is made of silicon carbide (SiC) with 400 grit, classified as super fine. The sheets were precisely cut into discs with a diameter of 25 mm, and pierced at the center to be fixed with an M6 screw onto a steel support. The support was clamped into a pneumatic rotary tool manufactured by Campbell Hausfeld, model TL102002, which operates at 25,000 rpm when supplied with 6.21 bar of pressure. The pneumatic rotary tool was secured to the worktable of a machining center using a vise. Figure 2 shows the brushing process setup of the prototype and main test end mills.

Figure 2. Polishing device configuration for the machining test end mill

In order to better understand the influence of the brushing process variables on the cutting edge, a systematic approach was developed, involving four distinct experimental stages. In this way, the results obtained in each stage guided the optimization of process settings in subsequent stages. Each test utilized distinct parameters for the brushing process. Table 2 presents the brushing settings parameters for each stage and tool.

Table 2. Brushing configuration parameters

Tool / Edge	Stage	Configuration	Abrasive	Grit	Brush Rotation Speed η (rpm)	Inclination of Disc Face Angle φ_b (°)	Contact Depth a_{pb} (mm)
P2/1	1	0	Al_2O_3	320	10,000	0	2
		1	Al_2O_3	320	10,000	0	2
		2	SiC	400	10,000	0	2
		3	Al_2O_3	320	10,000	5	3.5
P2/2	2	4	Al_2O_3	320	10,000	0	3.5
		5	Al_2O_3	320	6,000	0	3.5
		6	SiC	400	6,000	0	3.5
		7	SiC	400	10,000	5	3.5
P3/1	3	8	SiC	400	6,000	15	3
		9	Al_2O_3	320	6,000	15	3
		10	Al_2O_3	320	6,000	25	3
		11	SiC	400	6,000	25	3
P3/2	4	12	Al_2O_3	320	6,000	15	2.5
		13	SiC	400	6,000	15	2.5
		14	Al_2O_3	320	6,000	15	1
		15	SiC	400	6,000	15	1

Once the optimal configuration was determined based on optical and SEM micrographs alongside profile analysis to verify edge radius and rounding characteristics it was applied to the end mill designed for the machining tests. Subsequently, this optimized condition was compared against the tool without edge preparation.

3. Results

In this section, the microgeometries obtained from brushing tests using prototype end mills are presented. These microgeometries are evaluated in order to identify the optimal condition for implementation in the end mill to be employed in the machining tests. Subsequently, tool wear and workpiece surface finish are analyzed to understand the effects of the brushing process.

3.1 Abrasive Brushing Media

In order to have a better comprehension of the type brushing filaments and its impregnated micro-abrasive, a characterization through the SEM images was performed, as seen in Fig. 3. Upon examination of both sheets, the nylon filaments, along with the presence of micro-abrasives within them, were observed. A comparison between Al_2O_3 and SiC abrasives indicate

a substantial difference in their mechanical and physical properties. Both ceramics are employed in applications that require high wear and temperature resistance, due to the increased hardness (Munz; Fett, 1999).

Figure 3. SEM images of the brushing filaments and micro-abrasives

The micro-abrasive particles are randomly distributed over the surfaces of the filaments. The grains are irregularly shaped grains and vary in size. In the SiC sheets were observed larger grains with fewer sharp edges, formed by a greater number of unevenly arranged surfaces. On the other hand, the Al_2O_3 sheet is constituted of rounded grains that are more effectively deposited on the nylon filaments.

The grain size of the abrasive material is a determining factor in the shape and rate of material removal. Larger grains tend to increase the rate of material removal. In tests conducted by Denkena et al. (Denkena et al., 2008), which utilized the brushing process with different SiC grain sizes, it was found that a smaller grain size induced greater compressive stresses on the cutting edge. However, it also resulted in a reduction in the incidence of chipping and the surface roughness at the cutting edge.

3.2 Prototype Brushing Tests

In order to verify the influence of the brushing parameters and the micro-abrasive, a series of conditions were performed. One of the three tools (P1) maintained the edge condition from the manufacturing process. Figure 4 presents the characterization performed on the P1 mill.

Figure 4. Microgeometry of the unprepared P1 prototype mill

Measurements regarding the cutting edge were taken in terms of its shape and the size of the rounding. It is possible to see that the measured cutting edge radius r_β shows a value of 3.6 µm. This is considered to be a small radius given the diameter of the cutting tool. The observed edge condition was not adequate, as evidenced by the presence of grinding marks on both the rake face and flank face, summarized with the presence of edge chipping and burrs. That condition is attributed to the manufacturing process, as the grinding wheels make uneven contact with the tool substrate, thereby generating defects of this nature. Furthermore, poor edge quality can impair directly on tool performance and the quality of the workpiece surface. The subsequent process applied to the cutting tool has a significant impact on the state of the microgeometry (Meijner et al., 2024; Bouzakis et al., 2017).

At the initial stages of the brushing tests, the rotation speed of the brushing device was set 10,000 rpm, in order to preserve the integrity of the nylon filaments. By achieving a high rotation speed, the contact of the filaments on the cutting wedge results in an enhanced material removal that can alter the surface finishing. Moreover, the compressive residual stresses also increases as the brushing forces actuates on the edge (Stango, 2002). Figure 5 presents the microgeometry of the prepared sections and their respective edge characterization parameters.

In general, particles of the substrate were removed from the cutting edge, resulting in a convex surface with virtually no major defects or discontinuities, differing from that observer with the unprepared tool.

Figure 5. SEM micrographs of the microgeometry and contour measurement for the P2/1 tool

The region P2A1 was the first to be analyzed. Irregularities were observed on the flank face surface. Similarly, it was observed that the brushing process in the P2B1 region resulted in an edge discontinuity. This indicates that the material removal performed was not sufficient to correct this defect. However, analyses conducted prior to the brushing process showed that regions A and B of the edges, close to the corner, can present a greater number of defects and micro-chips.

A notable observation was the superior surface finishing in the regions P2C1 and P2D1 compared to the P2A1 and P2B1, attributed to the elimination of discontinuities. Also, the rounding $\bar{S}$ of the cutting edge for the configuration 2 was higher than the others conditions tested in the stage 1. The φ_b = 5° inclination in configuration 3 did not improve the symmetry of the rounding when compared to configuration 1, both tests utilizing the Al_2O_3 filament brush. In all the configurations of the stage 1 exhibited asymmetrical edge rounding (K < 1), not meeting the requirement of symmetrical rounding (K=1).

Considering that material removal by the filaments impregnated with micro-abrasives occurs through abrasion, the next step was the reduction in rotation speed and increase in contact depth. This was done in order to improve the contact time between the disc and the cutting edge. Figure 6 presents the results for the stage 2 of the brushing tests. In regard to the configuration 4 with Al_2O_3, was maintained the rotation speed of 10,000 rpm and the contact depth a_{pb} = 3.5 mm, while reducing the disc face angle to φ_b= 0°. About the contour it is possible to see that this configuration generated a light chamfer on the cutting edge, but with a moderate rounding.

Figure 6. SEM micrographs of the microgeometry and contour measurement for the P2/2 tool

For configuration 5, the strategy consisted of reducing the rotational speed to 6,000 rpm while maintaining the remaining brushing parameters unchanged. The edge rounding obtained in stage 2 was greater than that observed in the other configurations, as indicated by the larger value of $\bar{S}$. This condition directly affected the surface quality, which exhibited defects caused by material removal on the rake face.

A comparison between configurations 1 and 2, as well as configurations 3 and 7, in which only the abrasive type was varied, revealed that greater edge rounding $\bar{S}$ was achieved when the SiC brush was used. Furthermore, the K shape factor was higher for the configurations employing the SiC brush, although the values were still not close to the symmetry condition (K = 1). The modification of the brush inclination to φ_b = 5° did not result in improvements in either the edge rounding or the edge shape.

In phase 3, new configurations were proposed based on the observations obtained in the previous stages. The contact depth was reduced in order to minimize filament deformation as it advances over the cutting edge. This adjustment was intended to prevent excessive edge radius growth and to avoid a K shape factor tending toward 0. The brushing parameters and the resulting microgeometry are presented in Fig. 7.

Figure 7. SEM micrographs of the microgeometry and contour measurement for the P3/1 tool

To this purpose, new contact depth of a_{pb} = 3 mm was employed, and the rotation speed of 6,000 rpm was maintained. Two new disc angle of φ_b = 15° and φ_b = 25° were tested, since the prior angle, as in phase 1 and 2, did not result in significant differences on the microgeometries. According to Denkena et al. (Denkena et al., 2010), different inclinations can be used in the search for asymmetric rounding on the desired face. In this case, this technique was used to correct the asymmetry that occurs on the flank face.

The microgeometries generated in this phase had a lower surface quality than those obtained in phases 1 and 2. Nevertheless, the profiles showed lower rounding values for the flank section, which reduced the asymmetry effect of the previous phases. These results demonstrate that the inclination of the brush at φ_b = 25° did not have a significant influence when compared to the rounding generated at φ_b = 15°. Taking into account the brushing time, which was constant in all configurations, the φ_b = 25° could generate better results with a longer execution time. However, in this case, this inclination seemed excessive and did not generate greater rounding.

For phase 4, Figure 8 presents the combinations performed on tool P3, edge 2, and the respective results. The inclination angle φ_b = 15° was maintained, and new combinations were proposed. As verified in the previous phases, the rotation speed of 6,000 rpm was the suitable option, as the material removal was more controlled, which generated a moderate rounding. Furthermore, the edge quality was satisfactory, since no major chipping, burrs, or discontinuities were identified.

Figure 8. SEM micrographs of the microgeometry and contour measurement for the P3/2 tool

For configuration 12 and 13, the contact depth of a_{pb} = 2.5 mm was chosen to reduce the pressure imposed by the disc and reduce the rounding on the flank, obtained in phase 3. Analyzing the microgeometry generated by the configuration 12, it was possible to identify some imperfections. Although the grinding marks were eliminated, the brushing with Al_2O_3 filaments resulted in a rougher surface of the cutting edge, due to the detachment of WC grains from the substrate. These defects were more visible on the flank face. Considering that the edge region A generally has greater defects, it is believed that the material removal was insufficient for adequate preparation. In contrast, configuration 13, using the SiC brush, produced a better microgeometry than the previous configuration. Executions with this contact depth return similar preparations results even with the variation of abrasives, but the rounding presents a symmetry close to K = 1.

For the last configuration of the brushing tests, the approach was to reduce the contact depth of the brush filaments. As seen in the previous configurations, a greater contact depth led to increased material removal and, consequently, the size of the rounding. The shape of the rounding was also correlated to this parameter, and to achieve K = 1 the contact depth was set to a_{pb} = 1 mm. Moreover, according to Basset et al. (Basset et al., 2012), employing a contact depth between 1.25 and 1.50 mm would represent the limit for the radial use of SiC brushes.

Throughout the brushing test, the abrasive leaf discs were varied, which became a differential factor in the entire brushing test due to the behavior that can be observed in the preparations made with the Al_2O_3 abrasive brush. It can be observed that the carbide fracture occurred more frequently on the surface brushed with Al_2O_3, with grain detachment observed in some areas. This situation occurred less frequently when SiC abrasive was used. This directly influenced the final results of the preparation process. At the edge of the configuration 14, it is possible to visualize that, even with the rounding being moderate and its shape close to K = 1, the surface quality still has some imperfections. Contrarily, the cutting edge microgeometry of configuration 15 proved to be homogeneous, without defects or chipping. In addition, the rounding obtained was considered satisfactory, since the resulting shape factor was K = 0.98.

Another relevant observation concerns the surface quality obtained in phases 1 and 2. Configurations that presented greater rounding on the flank face exhibited a more homogeneous surface texture, which can be attributed to the increased removal of the WC substrate. Although these roundings showed good surface quality, their location along the tool wedge makes the edge preparations obtained in phases 1, 2, and 3 unsuitable. The profile evaluations indicated that the resulting edge roundings could be characterized by the junction of two distinct arcs, with the larger arc consistently located on the flank side.

In contrast, the profiles obtained in phase 4 demonstrated improved symmetry compared with the previous phases, with some profiles even showing a shift of the radius toward the rake face. Considering these observations, the configuration that best satisfied the requirements regarding cutting-edge surface quality, moderate edge rounding, and a shape factor close to 1 was configuration 15.

3.3 Main Cutting Tool Characterization

As verified in the brushing tests, several parameters were tested to determine the adequate combination to prepare the end mills destined to the machining tests. Configuration 15 was the suitable option, since it met the determined criteria for edge condition, rounding size and form factor K = 1. To better comprehend the impact of preparation by means of brushing, a SEM image of the two microgeometry conditions can be seen in Fig. 9.

Figure 9. End mill microgeometry and surface finish characterization using SEM

Similarly to what was observed for the unprepared prototype P1 end mill, the sharp condition exhibited several grinding marks originating from the manufacturing process. Although this condition presents a well-defined wedge geometry, some irregularities can be observed. At the cutting edge, micro-chipping and a serrated texture were identified. These characteristics are known to influence cutting stability, as the cutting edge represents a critical region that comes into direct contact with the workpiece material. Consequently, a high deviation in the measurements of the cutting edge radius and edge shape can be expected (Krebs et al., 2018).

Moreover, precise control over the edge rounding geometry is limited in this case, being primarily dictated by the mechanics of the grinding process. Studies such as Denkena et al. (Denkena et al., 2021) have demonstrated that the tool manufacturing process and its associated parameters directly affect the resulting microgeometry. In this context, the presence of surface defects was more pronounced in the unprepared tool.

Regarding the brushing process, the filaments containing SiC micro-abrasives proved to be effective in removing most of the grinding marks from both the rake face and the flank face. The material removal caused by the abrasive action of the filaments induces compressive stresses at the cutting edge, which can contribute positively to the wear resistance of the tool.

After the treatment, the cutting edge previously characterized by minimal rounding and classified as sharp presented greater uniformity, mainly due to the elimination of the serrated texture. This resulted in a refined and smoother microgeometry. Consequently, the edge radius r_β increased and a more symmetrical edge shape was achieved.

3.4 Cutting Tool Wear

In order to verify the impact of the brushing process on the cutting tool performance, a tool wear test was implemented. The main criteria for evaluation was the maximum flank wear VB_{MAX} = 0.20 mm for each microgeometry condition. In Figure 10, it is possible to verify the wear behavior curve for both conditions.

At the initial measurement, corresponding to 5.04 linear meters of cutting, the wear occurred in a similar manner. In the first instances of the cutting process, the wear rate is more accentuated, since the tool undergoes a period of adjustment to the specific cutting conditions. The two microgeometry conditions resulted in a flank wear close to 0.10 mm. Up to this point, the impact of edge preparation on the performance of the cutting tool has been relatively negligible.

Figure 10. Wear behavior curve of the uncoated end mills

In the subsequent linear meters of cutting, the wear rates occur differently for Sharp and Brushing conditions. It can be seen that the curve of the untreated tool resulted in greater flank wear than the brushed tool. This difference remained throughout the duration of the experiment. When reaching the tool life criterion of VB_{MAX} = 0.20 mm, the Sharp condition only machined 19.68 m, as the Brushing tool was able to achieve 23.88 m of linear cutting, which represents

an increment in tool life of 21.34 %. This summarizes the impact of the prepared tool. In the first instances of the cutting, the edge adapts itself to the thermo-mechanical loads imposed. Due to the enhanced mechanical resistance of fracture, the Brushing condition was more resistant to the wear than the untreated condition. The enhanced edge rounding, in this case, has been shown to have a substantial impact on the performance of cutting tools. The deviation of both conditions was considerably adequate, with no signs of abnormality.

In the experimental study conducted by Denkena et al. (Denkena et al., 2012) several radii sizes and shapes were compared utilizing the preparation method by brushing with SiC. The authors verified that the moderate rounding was the condition that most enhanced the tool life. Yet, the K factor impairs the wear behavior, in case of milling, $K > 1$ helps reduce flank wear when that is the predominant form of wear on the cutting tool. Wang et al. (Wang et al., 2020) confirmed that the brushing process increased the life of the cutting tool by 77%, among various preparation processes. The surface roughness of the rake face and cutting edge was also reduced, in comparison with the unprepared condition.

To evaluate the wear types and mechanisms presented on the cutting tool, optical images were taken at specific machining length of 5.04 m and 25.20 m, corresponding to the beginning and end of the cutting, seen in Figure 11.

Figure 11. Optical images of the end mills at cutting lengths of 5.04 m and 25.20 m

Regarding the rake face of both conditions, no abnormal wear or defects were detected that could adversely affect the performance of the cutting tool. Despite the end mill employed in the tests being uncoated, no crater wear KT was identified throughout the cutting. It has been observed at the flank face that micro-chipping of the cutting edge has occurred. This phenomenon occurred in the sharp end mills, at the end of the first 5.04 m machined. In the subsequent machined length, no micro-chipping was observed on edges that did not previously have it. However, the size of the micro-chipping increased with the progression of the wear test.

For the brushed condition, micro-chipping was observed only when the tool passed the end of life criterion, ensuring the effectiveness of the preparation process in controlling the tool damage within the cutting. The flank wear land band was more regular than the Sharp condition, exhibiting less irregularities and defects. In the study of Zeilmann et al. (Zeilmann et al., 2026), when machining AISI P20 steel with drag finish prepared end mills also verified that the enhancement of the edge rounding helped the cutting tool to have a better control of wear behavior and not experienced chipping on the cutting edge. Also, Rech et al. (Rech et al., 2005) verified that in milling inserts with edge preparation, the width of flank wear was consistent along the edge, which contributed to its improved cutting performance.

In both conditions it was possible to identify the main wear mechanism of abrasion. Adhesion was also present, assessed through SEM images. No other wear mechanisms were noted. The tests performed by Barbosa et al. (Barbosa et al., 2021) with unprepared and prepared end mills when machining a similar workpiece material and cutting conditions, also resulted in an increment of tool life for the treated tools. The same wear mechanism was identified.

3.5 Surface Quality and Roughness

The surface quality of the workpiece generated during the machining test was evaluated using texture images and roughness measurements, in conjunction with their profiles. This characterization was performed in order to compare the results obtained for each condition. Figure 12 shows the representative textures and roughness profiles are displayed for the beginning and end of the life of the sharp and brushed end mills, in addition to the average roughness values.

Fig. 12 Roughness profiles and parameters with surface topography of the workpiece measured at cutting lengths of 0 m and 25.20 m

As the end mills are used, tool wear progressively increases, causing continuous changes in the cutting edge within the working region. Consequently, the surface generated during machining does not exhibit a uniform texture throughout the entire process. In both tested conditions, similar surface textures were observed at the beginning of machining, where the first tool passes produced well-defined cutting marks with a consistent pattern. However, when analyzing the texture after 25.20 linear meters of cutting, noticeable differences were identified. The previously pronounced marks and clearly defined grooves were no longer evident. In the machining of Inconel 718, Fontanive et al. (Fontanive et al., 2019) also reported that new end mills generate a well-defined texture, whereas worn tools tend to produce surfaces with material adhered to the workpiece.

The roughness profiles obtained for both tested conditions show typical behavior at 0 m of linear cutting, characterized by well-defined peaks and valleys with constant spacing between them. In contrast, at the end of the machining test, the profiles differ considerably along the evaluated section. As the tool loses its cutting efficiency, the material removal mechanism shifts from shearing to increased plastic deformation. This effect presses the removed material onto the workpiece surface, resulting in a more irregular surface profile.

Regarding the Ra roughness parameter, the measured values for both 0 m and 25.20 linear meters of cutting were lower for the brushed condition. This behavior can be explained by the small edge radius present at the corners of the end mills, which plays an important role in the resulting surface quality. The edge radius softens the tool marks generated during machining. This radius begins on the cylindrical side of the end mill and extends to the top face, exhibiting an asymmetric profile characterized by a shape factor $K<1$. According to Maiss et al. (Maiss et al., 2017), this type of rounding promotes greater plastic deformation of the machined material, which contributes to the reduction of surface roughness.

For the Rz roughness parameter, it was also observed that the brushed condition resulted in lower values both at the beginning of cutting and at the end of tool life. Another contributing factor was the lower incidence of micro-chipping on the prepared edges compared with the sharp tool, which resulted in reduced wear and consequently lower roughness values. However,

for the Rz1max parameter, higher values were obtained for the brushed condition. This behavior can be attributed to the larger edge radius, which may promote a ploughing effect at the cutting edge. In this case, the material is plastically deformed and pushed against the workpiece surface rather than being completely removed. Overall, the measured roughness values are slightly lower for the brushed condition, both at the beginning and at the end of the tool life.

4. Conclusions

The brushing process is widely used in the industry, due to its effectiveness in treating different types of cutting tools, low costs of implementation and relatively short operation times. This study enables a comparative analysis of the various configurations of the brushing process parameters and their direct impacts on the resulting microgeometry, tool wear, and surface quality of the machined part. The main conclusions of the study were:

Brushing process parameters directly govern the generated cutting edge microgeometry; specifically, the brush angle dictates the rounding shape, while the contact depth significantly impacts both its size and final profile. Additionally, the brush rotational speed acts as a determining factor for the material removal rate. Although specific parameter combinations induced minor edge irregularities that could compromise cutting stability, the application of silicon carbide (SiC) micro-abrasive surface sheets proved highly effective, yielding satisfactory, defect-free microgeometries in most cases. Among the tested variations, "configuration 15" produced the most adequate rounding size and shape for subsequent machining implementation.

In machining tests, it was observed that the brushed tool exhibited less flank wear compared to the untreated tool. When flank wear VB_{MAX} = 0.2 mm was reached, the increase in the life of the brushed tool was more than 21%. Although the wear types and wear mechanisms were similar in both conditions, the brushing condition was capable of adequately controlling them.

Finally, the investigation focused on the surface quality of the workpiece revealed that the brushing condition resulted in a reduction in Ra and Rz roughness both at the beginning and at the end of the end mill life, in comparison with the Sharp tool. In the case of the Rz1max parameter, the untreated tool obtained lower values than the brushed tool. The optical visualization of the texture generated in the machining process also corroborates this fact.

Acknowledgments

The authors would like to thank the University of Caxias do Sul and OTEC GmbH (Germany) for providing the resources necessary to conduct this research. The authors also acknowledge Secta Tools for supplying the cutting tools used in this study. In addition, the authors gratefully acknowledge the financial support and scholarships provided by CAPES and CNPq.

Authors Contributions

All authors contributed to the study conception and design.

Statements & Declarations

Funding: This work was supported by William Buckel, Luccas A P Delgado, Rodrigo P Zeilmann and University of Caxias do Sul.

Competing Interests: The authors have no relevant financial or non-financial interests to disclose.

References

[1] Toenshoff, H. K., & Denkena, B. (2013). Basics of cutting and abrasive processes.

[2] Wegener, K., Kuster, F., Weikert, S., Weiss, L., & Stirnimann, J. (2016). Success Story Cutting. Procedia CIRP, 46, 512–524. https://doi.org/10.1016/j.procir.2016.04.110

[3] Denkena, B., & Biermann, D. (2014). Cutting edge geometries. *CIRP Annals - Manufacturing Technology*, *63*(2), 631–653. https://doi.org/10.1016/j.cirp.2014.05.009

[4] Tikal, F. (Ed.). (2009). *Schneidkantenpräparation: Ziele, Verfahren und Messmethoden: Berichte aus Industrie und Forschung*. Kassel University press GmbH.

[5] Denkena, B., Köhler, J., & Ventura, C. E. H. (2013). Customized cutting edge preparation by means of grinding. *Precision Engineering*, *37*(3), 590–598. https://doi.org/10.1016/j.precisioneng.2013.01.004

[6] Denkena, B., Lucas, A., & Bassett, E. (2011). Effects of the cutting edge microgeometry on tool wear and its thermo-mechanical load. *CIRP Annals - Manufacturing Technology*, *60*(1), 73–76. https://doi.org/10.1016/j.cirp.2011.03.098

[7] Zhuang, K., Fu, C., Weng, J., & Hu, C. (2021). Cutting edge microgeometries in metal cutting: a review. *International Journal of Advanced Manufacturing Technology*, *116*(7–8), 2045–2092. https://doi.org/10.1007/s00170-021-07558-6

[8] Denkena, B., Becker, J. C., & de Leon-Garcia, L. (2005). Study of the influence of the cutting edge microgeometry on the cutting forces and wear behavior in turning operations. In *Proceedings of the 8th CIRP, International Workshop on Modelling of Machining Operations, Chemnitz, Germany*, 503-507.

[9] Stango, R. J. (2002). Filamentary brushing tools for surface finishing applications. *Metal Finishing*, *100*, 82-91. https://doi.org/10.1016/S0026-0576(02)82007-4

[10] Overholser, R. W., Stango, R. J., & Fournelle, R. A. (2003). Morphology of metal surface generated by nylon/abrasive filament brush. *International Journal of Machine Tools and Manufacture*, *43*(2), 193–202. https://doi.org/10.1016/S0890-6955(02)00112-8

[11] Rodríguez, C. (2009). Cutting edge preparation of precision cutting tools by applying micro-abrasive jet machining and brushing. In *Kassel University Press GmbH*.

[12] Denkena, B., De Leon, L., & Rehe, M. (2009). Prozesssicher verrunden - Bürstkinematik und Borstenverschleiß bei der Schneidkantenpräparation. *Werkstatt Und Betrieb*, *10*, 36–39.

[13] Bergs, T., Schneider, S. A. M., Amara, M., & Ganser, P. (2020). Preparation of symmetrical and asymmetrical cutting edges on solid cutting tools using brushing tools with filament-integrated diamond grits. *Procedia CIRP*, *93*(March), 873–878. https://doi.org/10.1016/j.procir.2020.04.028

[14] Frank, P., & Otto, A. (2019). Flakkotieren von Fräsern zum Mikro-Hartfräsen - Optimierung des Einsatzverhaltens von Mikrotorusfräsern beim Hartfräsen durch Hochpräzisionsbürsten. *WT Werkstattstechnik*, *109*(11–12), 833–839.

[15] Breidenstein, B., Vogel, N., & Bergmann, B. (2024). Influence of the preparation processes on the residual stresses in PCD and PcBN tools. *European Journal of Materials*, *4*(1). https://doi.org/10.1080/26889277.2024.2350936

[16] Zeilmann, R. P., Ost, C. A., & Fontanive, F. (2018). Characterization of edge preparation processes and the impact on surface integrity after milling of AISI P20 steel. *Journal of the Brazilian Society of Mechanical Sciences and Engineering*, *40*(9), 1–7. https://doi.org/10.1007/s40430-018-1338-7

[17] Bouzakis, K. D., Bouzakis, E., Kombogiannis, S., Makrimallakis, S., Skordaris, G., Michailidis, N., Charalampous, P., Paraskevopoulou, R., M'Saoubi, R., Aurich, J. C., Barthelmä, F., Biermann, D., Denkena, B., Dimitrov, D., Engin, S., Karpuschewski, B., Klocke, F., Özel, T., Poulachon, G., … Zeman, P. (2014). Effect of cutting edge preparation of coated tools on their performance in milling various materials. *CIRP Journal of Manufacturing Science and Technology*, *7*(3), 264–273. https://doi.org/10.1016/j.cirpj.2014.05.003

[18] Denkena, B., Friemuth, T., Fedorenko, S., & Groppe, M. (2002). An der Schneide wird das Geld verdient. *Werkzeugtechnik+ Verfahren*, *30*(12), 24-26.

[19] Munz, D; Fett, T. (1999). Ceramics: Mechanical Properties, Failure Behavior, Materials Selection. Springer Berlin Heidelberg,

[20] Denkena, B., Leon-Garcia, L., & Bassett, E. (2008). Preparation of designed cutting edge microgeometries by simultaneous 5-axes brushing. In *Proceedings of the 3rd International Conference on Manufacturing Engineering (ICMEN) and EUREKA Brokerage Event,* 1(3), 117–123.

[21] Meijer, A. L., Lopes Dias, N. F., Tillmann, W., & Biermann, D. (2024). Preparation of asymmetrical cutting edge geometries on micro end mills using pressurized wet abrasive jet machining for hard micromachining of AISI M3:2. *CIRP Journal of Manufacturing Science and Technology*, *51*(May), 252–262. https://doi.org/10.1016/j.cirpj.2024.05.005

[22] Bouzakis, K. D., Charalampous, P., Kotsanis, T., Skordaris, G., Bouzakis, E., Denkena, B., Breidenstein, B., Aurich, J. C., Zimmermann, M., Herrmann, T., & M'saoubi, R. (2017). Effect of HM substrates' cutting edge roundness manufactured by laser machining and micro-blasting on the coated tools' cutting performance. *CIRP Journal of Manufacturing Science and Technology*, *18*, 188–197. https://doi.org/10.1016/j.cirpj.2017.02.003

[23] Bassett, E., Köhler, J., & Denkena, B. (2012). On the honed cutting edge and its side effects during orthogonal turning operations of AISI1045 with coated WC-Co inserts. *CIRP Journal of Manufacturing Science and Technology*, *5*(2), 108–126. https://doi.org/10.1016/j.cirpj.2012.03.004

[24] Denkena, B., De León, L., Bassett, E., & Rehe, M. (2010). Cutting edge preparation by means of abrasive brushing. *Key Engineering Materials*, *438*, 1–7. https://doi.org/10.4028/www.scientific.net/KEM.438.1

[25] Krebs, E., Wolf, M., Biermann, D., Tillmann, W., & Stangier, D. (2018). High-quality cutting edge preparation of micromilling tools using wet abrasive jet machining process. *Production Engineering*, *12*(1), 45–51. https://doi.org/10.1007/s11740-017-0787-7

[26] Denkena, B., Krödel-Worbes, A., Beblein, S., & Hein, M. (2021). Influence of end mill manufacturing on cutting edge quality and wear behavior. *Journal of Manufacturing and Materials Processing*, *5*(3), 77.Denkena, B., De León, L., Bassett, E., & Rehe, M. (2010). Cutting edge preparation by means of abrasive brushing. *Key Engineering Materials*, *438*, 1–7. https://doi.org/10.4028/www.scientific.net/KEM.438.1

[27] Zeilmann, R.P., Delgado, L.A.P. & Subtil, J.L.N. Effect of cutting edge preparation by drag finishing on the tool wear in milling of steel. *Int J Adv Manuf Technol* (2026). https://doi.org/10.1007/s00170-025-17307-8

[28] Denkena, B., Koehler, J., & Rehe, M. (2012). Influence of the honed cutting edge on tool wear and surface integrity in slot milling of 42CrMo4 steel. *Procedia CIRP*, *1*(1), 190–195. https://doi.org/10.1016/j.procir.2012.04.033

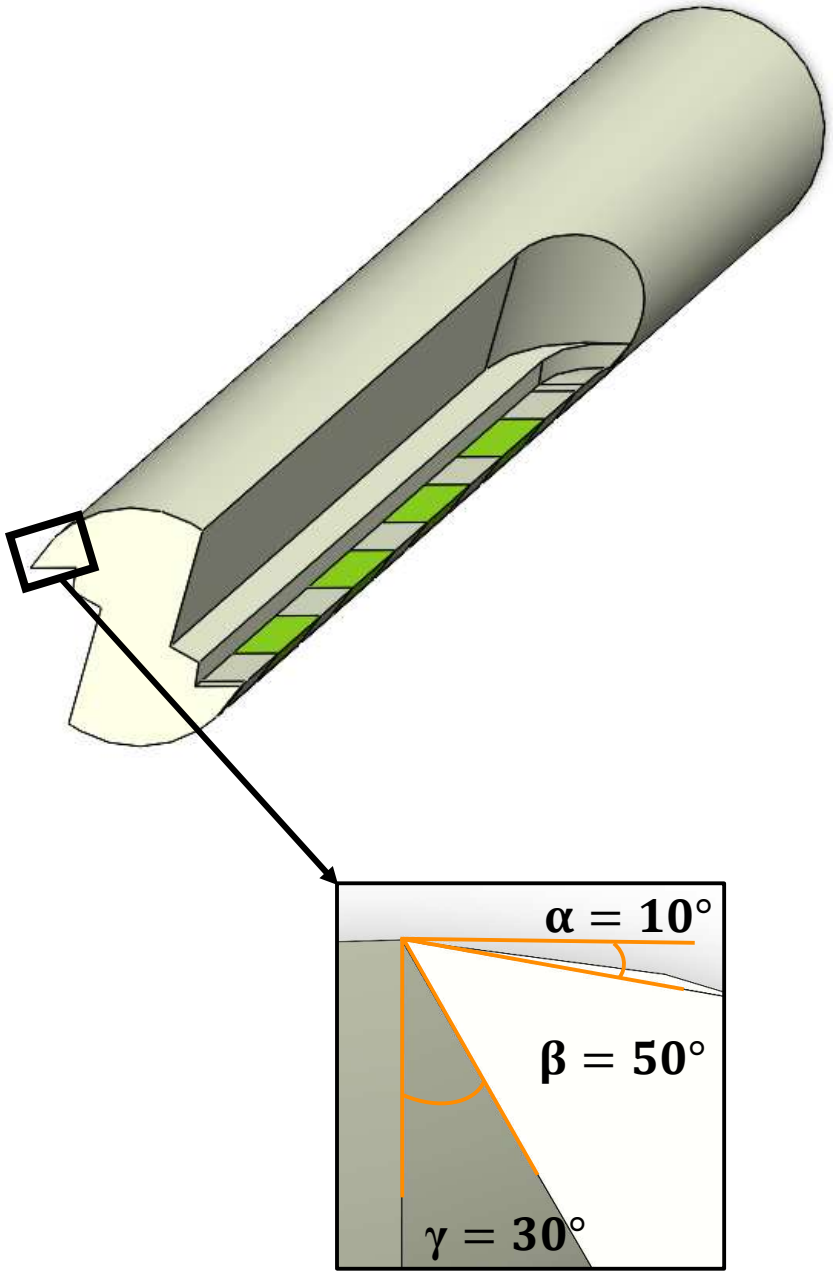
[29] Wang, W., Saifullah, M. K., Aßmuth, R., Biermann, D., Arif, A. F. M., & Veldhuis, S. C. (2020). Effect of edge preparation technologies on cutting edge properties and tool performance. *International Journal of Advanced Manufacturing Technology*, *106*(5–6), 1823–1838. https://doi.org/10.1007/s00170-019-04702-1

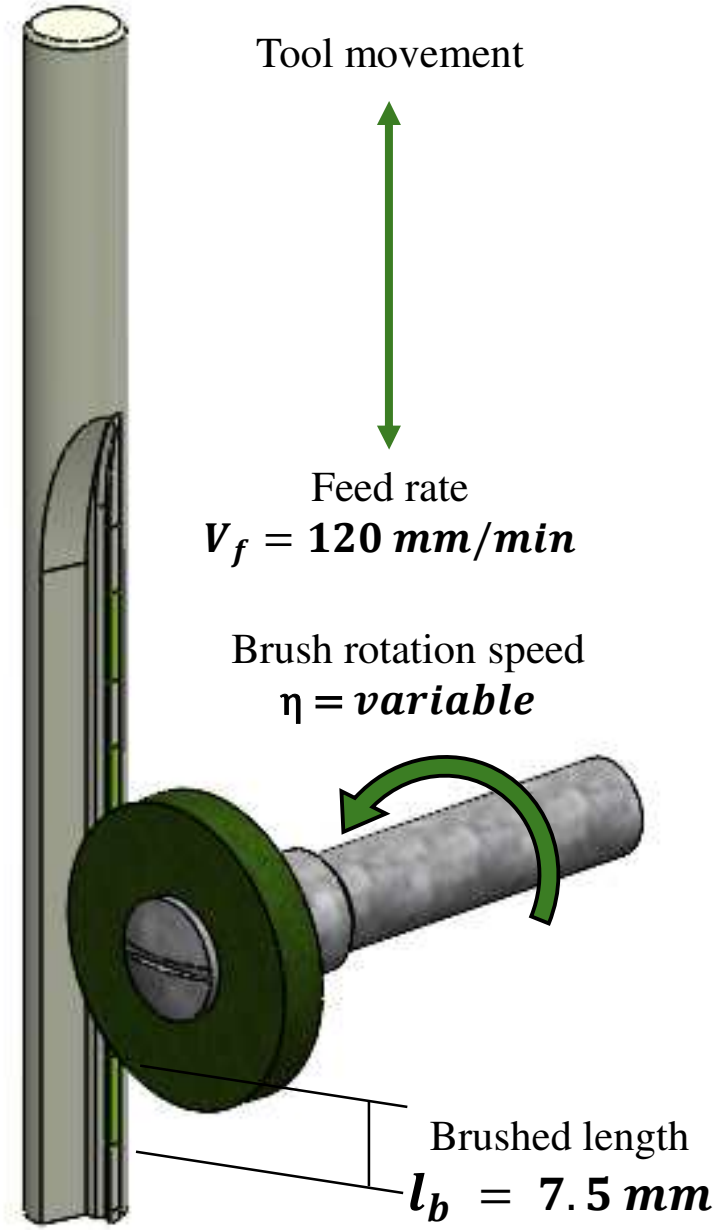
[30] Rech, J., Yen, Y. C., Schaff, M. J., Hamdi, H., Altan, T., & Bouzakis, K. D. (2005). Influence of cutting edge radius on the wear resistance of PM-HSS milling inserts. *Wear*, *259*(7–12), 1168–1176. https://doi.org/10.1016/j.wear.2005.02.072

[31] Barbosa, M. G. C. B., Hassui, A., & de Oliveira, P. A. (2021). Effect of cutting parameters and cutting edge preparation on milling of VP20TS steel. *International Journal of Advanced Manufacturing Technology*, *116*(9–10), 2929–2942. https://doi.org/10.1007/s00170-021-07654-7

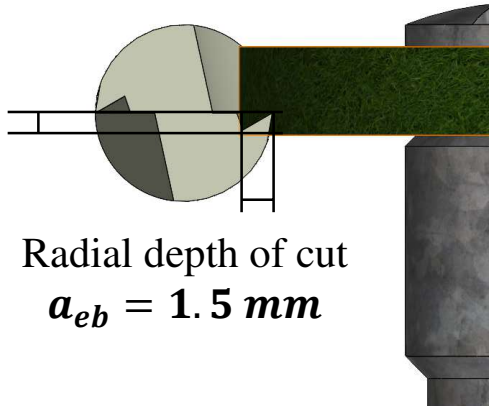
[32] Fontanive, F., Zeilmann, R. P., & Schenkel, J. D. (2019). Surface quality evaluation after milling Inconel 718 with cutting edge preparation. *International Journal of Advanced Manufacturing Technology*, *104*(1–4), 1087–1098. https://doi.org/10.1007/s00170-018-03260-2

[33] Maiss, O., Grove, T., & Denkena, B. (2017). Influence of asymmetric cutting edge roundings on surface topography. *Production Engineering*, *11*(4–5), 383–388. https://doi.org/10.1007/s11740-017-0742-7



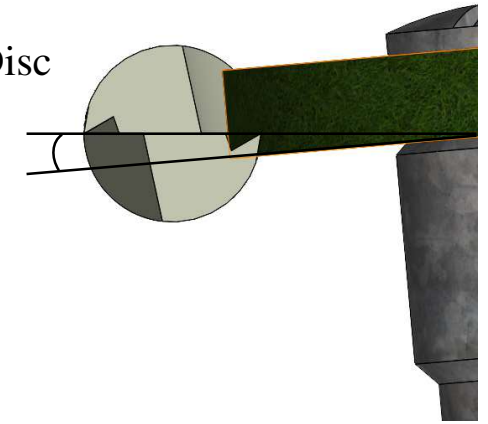


Axial depth of cut /
Contact depth
$a_{pb} = variable$



Radial depth of cut
$a_{eb} = 1.5\ mm$

Inclination of Disc
Face Angle
$\varphi_b = variable$

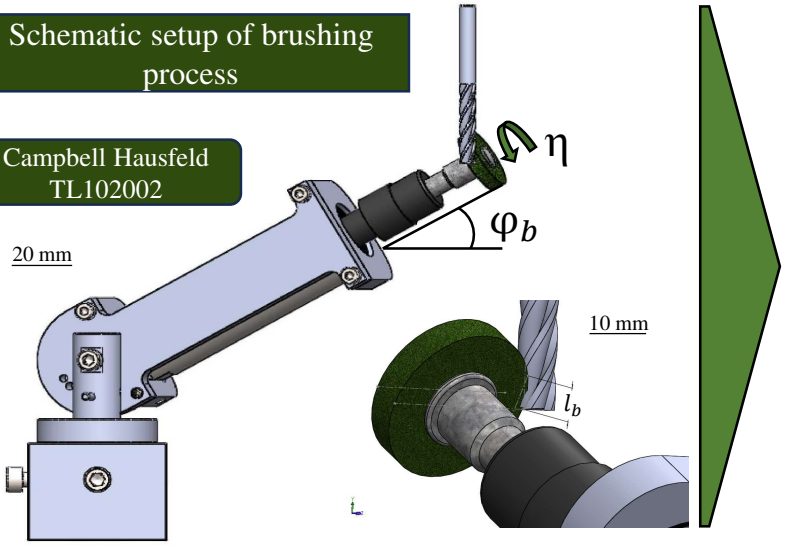


Abrasive disc
$Diameter = 25\ mm$
$Abrasive = variable$

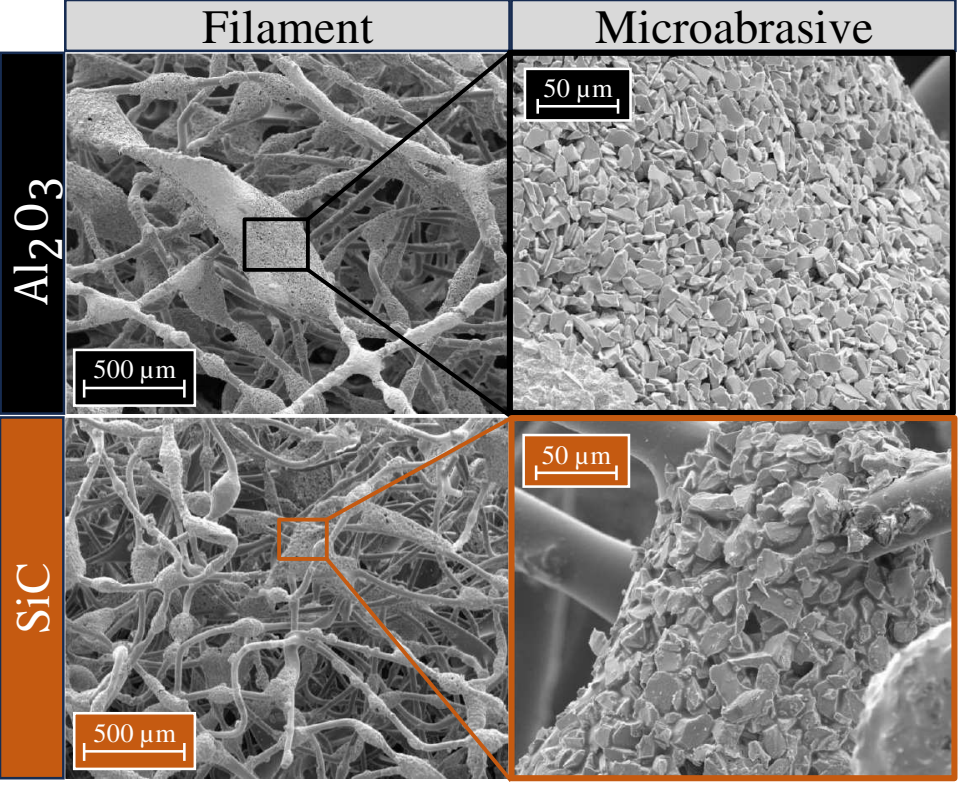


Schematic setup of brushing process

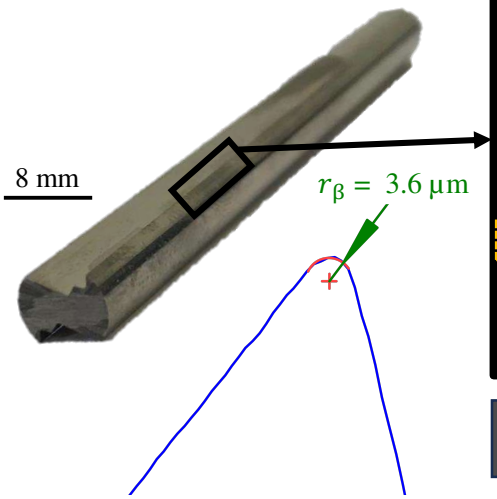
Campbell Hausfeld TL102002

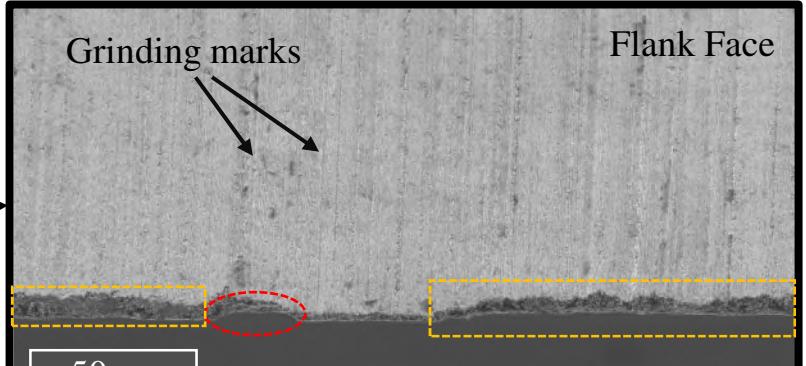





Filament
Microabrasive
Al_2O_3
SiC
500 µm
50 µm
500 µm
50 µm

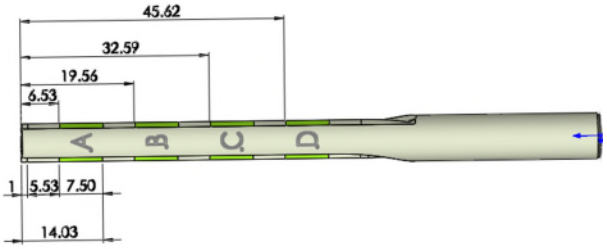
Prototype Mill 1 – P1B1

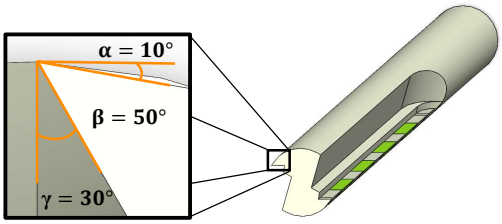




S_α = 7.8 µm S_γ = 6.2 µm $\bar{S}$ = 7.0 um K = 0.79

Mahr MarTalk - Contour Measure	Measured Length: 2.00 mm	2000 Points Acquired

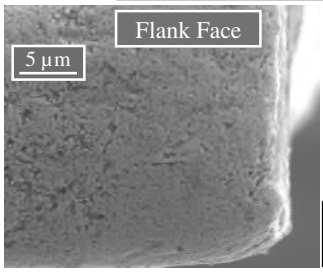


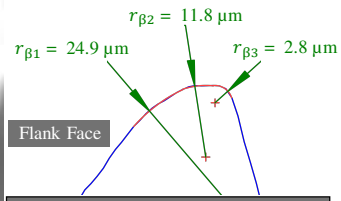


P2A1 No. 0

v_c = 13.1 m/s
v_f = 120 mm/min
φ_b = 0°
t = 60 s

a_{pb} = 2 mm
a_{eb} = 1.5 mm
l_b = 7.5 mm
Abrasive: Al_2O_3 #320



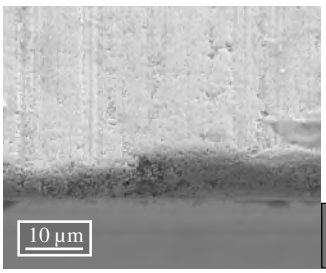


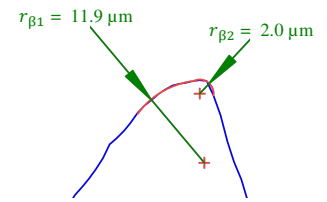
S_α = 20.7 µm S_γ = 12.0 µm
$\bar{S}$ = 16.4 µm K = 0.57

P2B1 No. 1

v_c = 13.1 m/s
v_f = 120 mm/min
φ_b = 0°
t = 60 s

a_{pb} = 2 mm
a_{eb} = 1.5 mm
l_b = 7.5 mm
Abrasive: Al_2O_3 #320



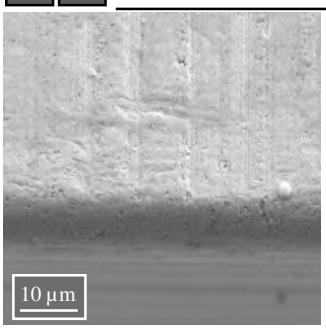


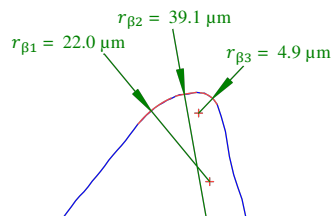
S_α = 17.2 µm S_γ = 7.9 µm
$\bar{S}$ = 12.5 µm K = 0.46

P2C1 No. 2

v_c = 13.1 m/s
v_f = 120 mm/min
φ_b = 0°
t = 60 s

a_{pb} = 2 mm
a_{eb} = 1.5 mm
l_b = 7.5 mm
Abrasive: SiC #400



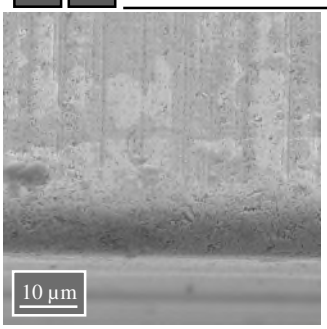


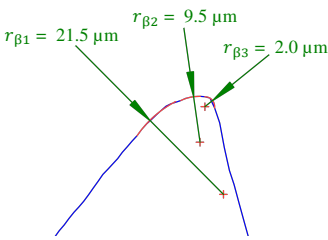
S_α = 22.4 µm S_γ = 14.8 µm
$\bar{S}$ = 18.6 µm K = 0.66

P2D1 No. 3

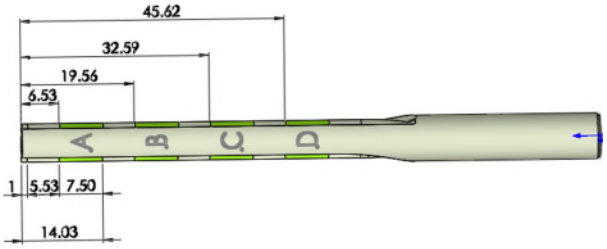
v_c = 13.1 m/s
v_f = 120 mm/min
φ_b = 5°
t = 60 s

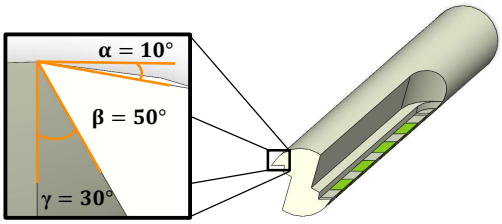
a_{pb} = 3.5 mm
a_{eb} = 1.5 mm
l_b = 7.5 mm
Abrasive: Al_2O_3 #320





S_α = 22.4 µm S_γ = 11.5 µm
$\bar{S}$ = 16.9 µm K = 0.51

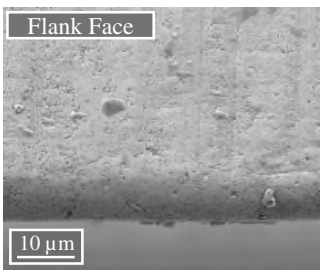


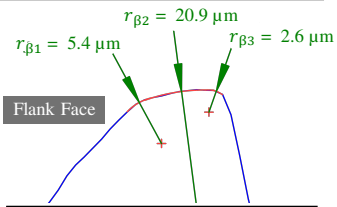


P2A2 No. 4

v_c = 13.1 m/s
v_f = 120 mm/min
φ_b = 0°
t = 60 s

a_{pb} = 3.5 mm
a_{eb} = 1.5 mm
l_b = 7.5 mm
Abrasive: Al_2O_3 #320



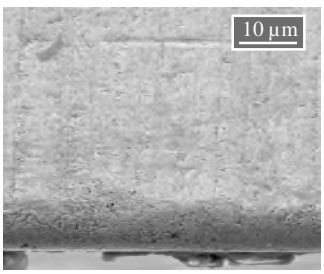


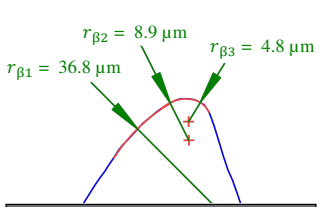
S_α = 17.7 µm S_γ = 11.9 µm
$\bar{S}$ = 14.8 µm K = 0.67

P2B2 No. 5

v_c = 7.9 m/s
v_f = 120 mm/min
φ_b = 0°
t = 60 s

a_{pb} = 3.5 mm
a_{eb} = 1.5 mm
l_b = 7.5 mm
Abrasive: Al_2O_3 #320



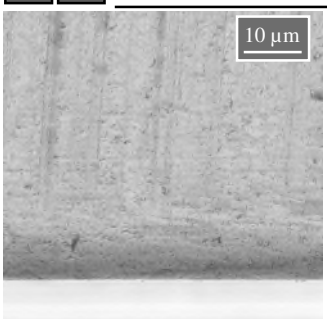


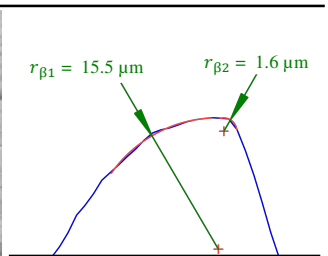
S_α = 28.2 µm S_γ = 15.1 µm
$\bar{S}$ = 21.6 µm K = 0.53

P2C2 No. 6

v_c = 7.9 m/s
v_f = 120 mm/min
φ_b = 0°
t = 60 s

a_{pb} = 3.5 mm
a_{eb} = 1.5 mm
l_b = 7.5 mm
Abrasive: SiC #400



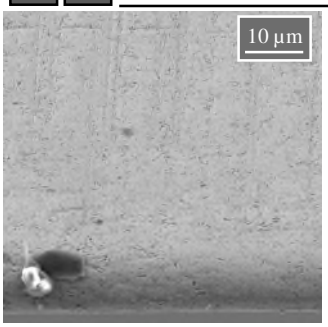


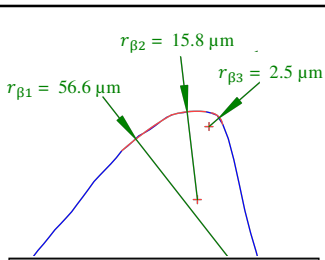
S_α = 19.9 µm S_γ = 11.7 µm
$\bar{S}$ = 15.8 µm K = 0.59

P2D2 No. 7

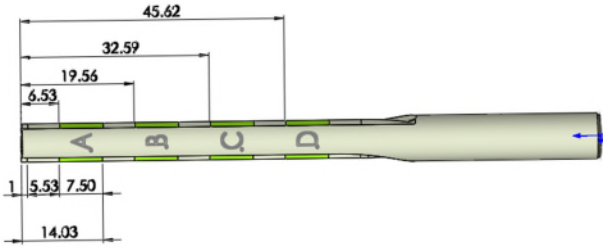
v_c = 13.1 m/s
v_f = 120 mm/min
φ_b = 5°
t = 60 s

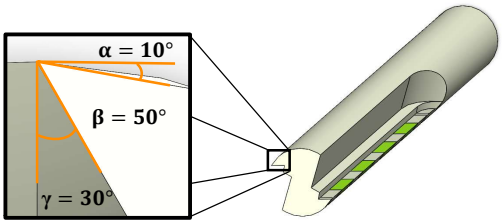
a_{pb} = 3.5 mm
a_{eb} = 1.5 mm
l_b = 7.5 mm
Abrasive: SiC #400





S_α = 23.7 µm S_γ = 14.2 µm
$\bar{S}$ = 18.9 µm K = 0.60

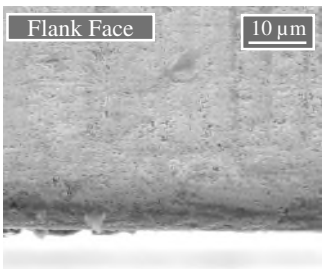


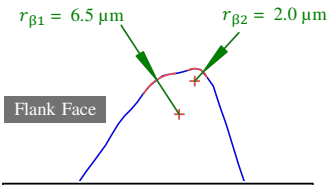


P3A1 — No. 8

v_c = 7.9 m/s
v_f = 120 mm/min
φ_b = 15°
t = 60 s

a_{pb} = 3 mm
a_{eb} = 1.5 mm
l_b = 7.5 mm
Abrasive: SiC #400



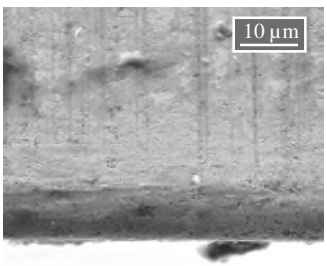


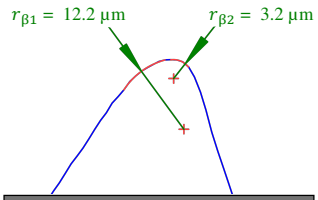
S_α = 17.5 µm S_γ = 10.3 µm
$\bar{S}$ = 13.6 µm K = 0.59

P3B1 — No. 9

v_c = 7.9 m/s
v_f = 120 mm/min
φ_b = 15°
t = 60 s

a_{pb} = 3 mm
a_{eb} = 1.5 mm
l_b = 7.5 mm
Abrasive: Al_2O_3 #320



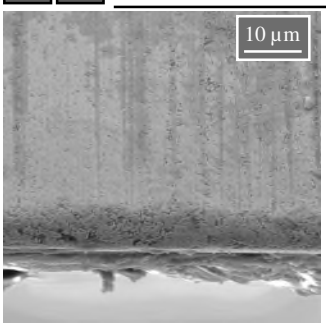


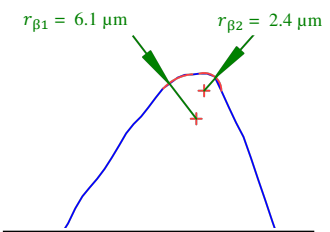
S_α = 18.3 µm S_γ = 11.4 µm
$\bar{S}$ = 14.8 µm K = 0.62

P3C1 — No. 10

v_c = 7.9 m/s
v_f = 120 mm/min
φ_b = 25°
t = 60 s

a_{pb} = 3 mm
a_{eb} = 1.5 mm
l_b = 7.5 mm
Abrasive: Al_2O_3 #320



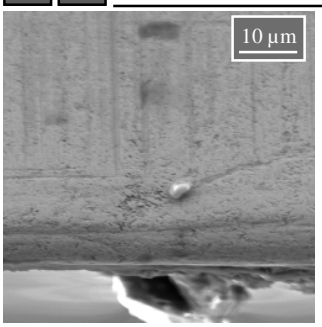


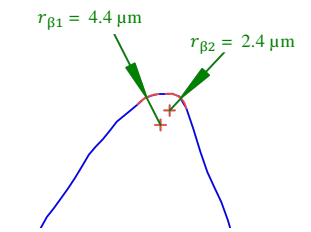
S_α = 16.3 µm S_γ = 14.2 µm
$\bar{S}$ = 15.2 µm K = 0.87

P3D1 — No. 11

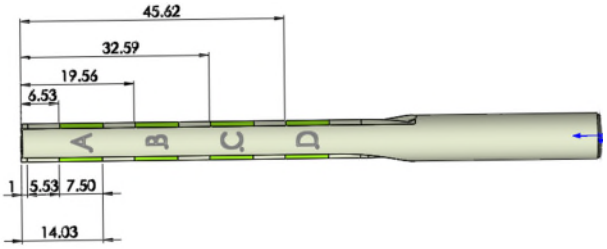
v_c = 7.9 m/s
v_f = 120 mm/min
φ_b = 25°
t = 60 s

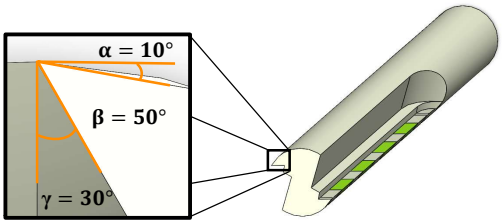
a_{pb} = 3 mm
a_{eb} = 1.5 mm
l_b = 7.5 mm
Abrasive: SiC #400





S_α = 18.0 µm S_γ = 9.9 µm
$\bar{S}$ =14.0 µm K = 0.55

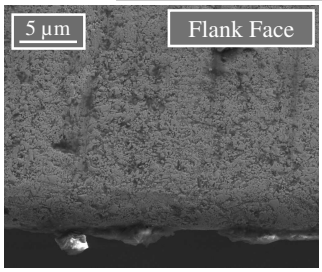


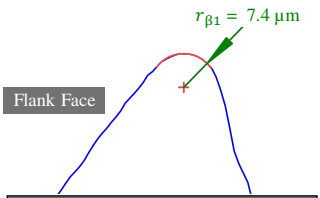


P3A2 No. 12

v_c = 7.9 m/s
v_f = 120 mm/min
φ_b = 15°
t = 60 s

a_{pb} = 2.5 mm
a_{eb} = 1.5 mm
l_b = 7.5 mm
Abrasive: Al_2O_3 #320



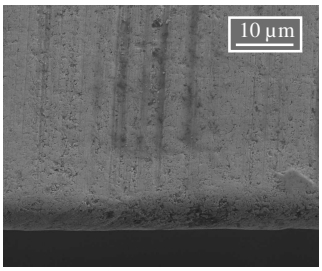


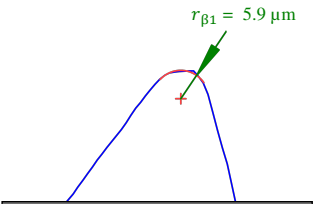
S_α = 16.3 µm S_γ = 13.9 µm
$\bar{S}$ = 15.1 µm K = 0.85

P3B2 No. 13

v_c = 7.9 m/s
v_f = 120 mm/min
φ_b = 15°
t = 60 s

a_{pb} = 2.5 mm
a_{eb} = 1.5 mm
l_b = 7.5 mm
Abrasive: SiC #400



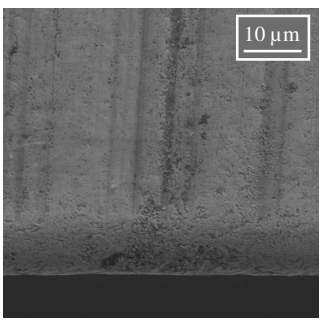


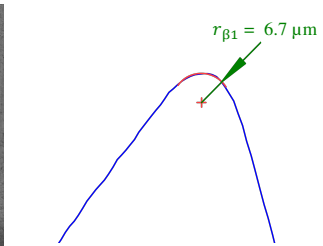
S_α = 12.2 µm S_γ = 10.9 µm
$\bar{S}$ = 13.6 µm K = 0.89

P3C2 No. 14

v_c = 7.9 m/s
v_f = 120 mm/min
φ_b = 15°
t = 60 s

a_{pb} = 1 mm
a_{eb} = 1.5 mm
l_b = 7.5 mm
Abrasive: Al_2O_3 #320



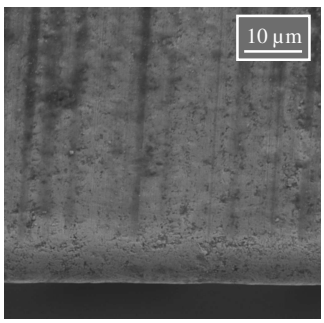


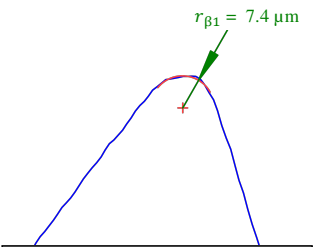
S_α = 16.8 µm S_γ = 16.1 µm
$\bar{S}$ = 16.4 µm K = 0.96

P3D2 No. 15

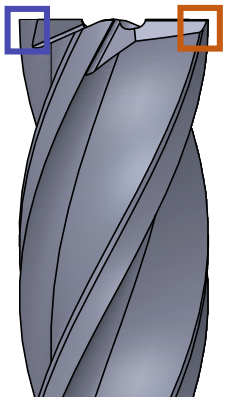
v_c = 7.9 m/s
v_f = 120 mm/min
φ_b = 15°
t = 60 s

a_{pb} = 1 mm
a_{eb} = 1.5 mm
l_b = 7.5 mm
Abrasive: SiC #400





S_α = 16.6 µm S_γ = 16.2 µm
$\bar{S}$ = 16.4 µm K = 0.98



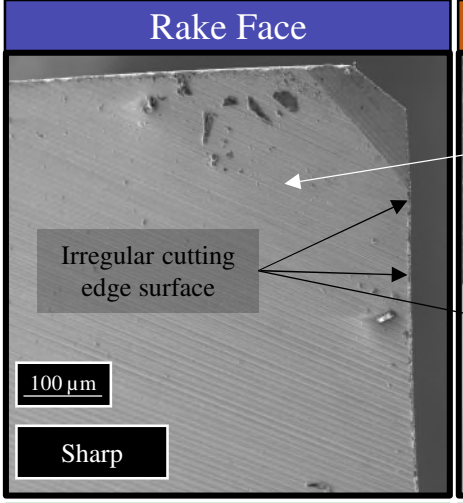
Tool: WC K40 10% Co End Mill

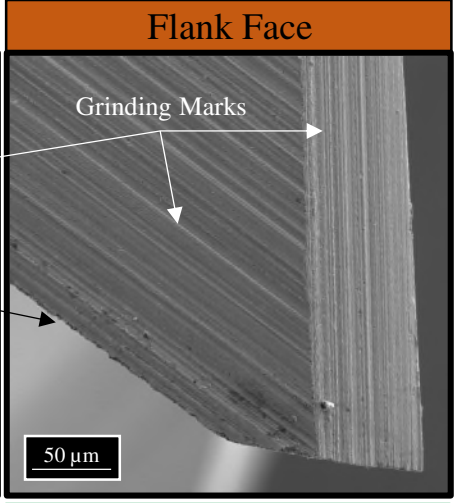
Clearance Angle:	$\alpha = 10°$
Rake Angle:	$\gamma = 8°$
Wedge Angle:	$\beta = 72°$
Helix Angle:	$\lambda = 30°$

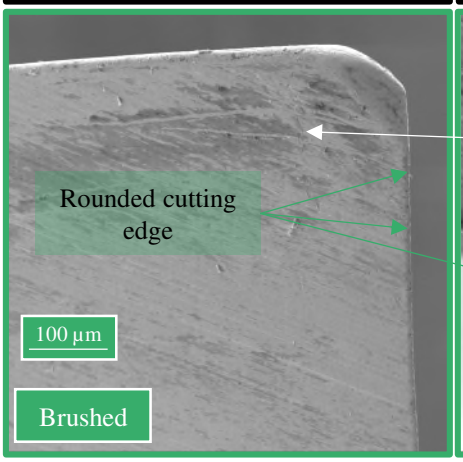


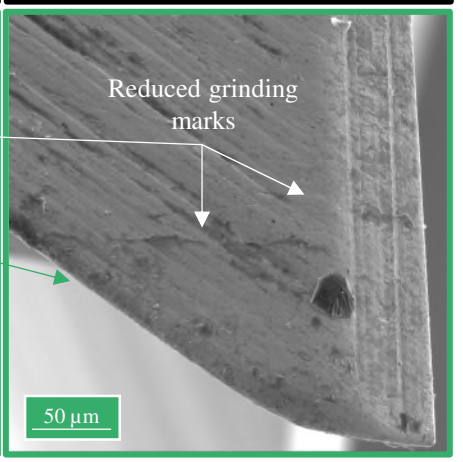
Brushing Parameters: Config. 15

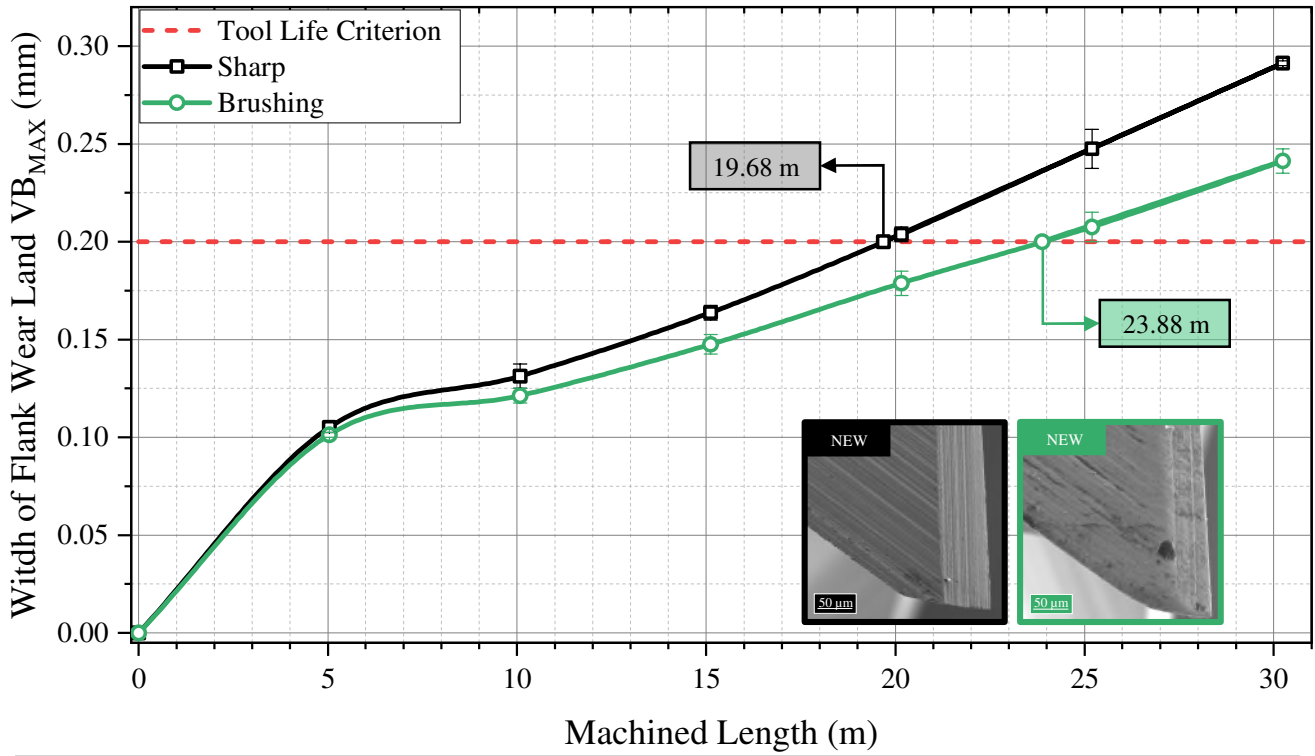
$v_c = 7.9$ m/s	$a_{pb} = 1$ mm
$v_f = 120$ mm/min	$a_{eb} = 1.5$ mm
$\varphi_b = 15°$	$l_b = 5.3$ mm
t = 60 s	Abrasive: SiC #400





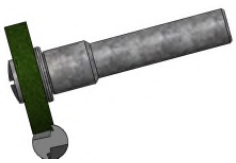






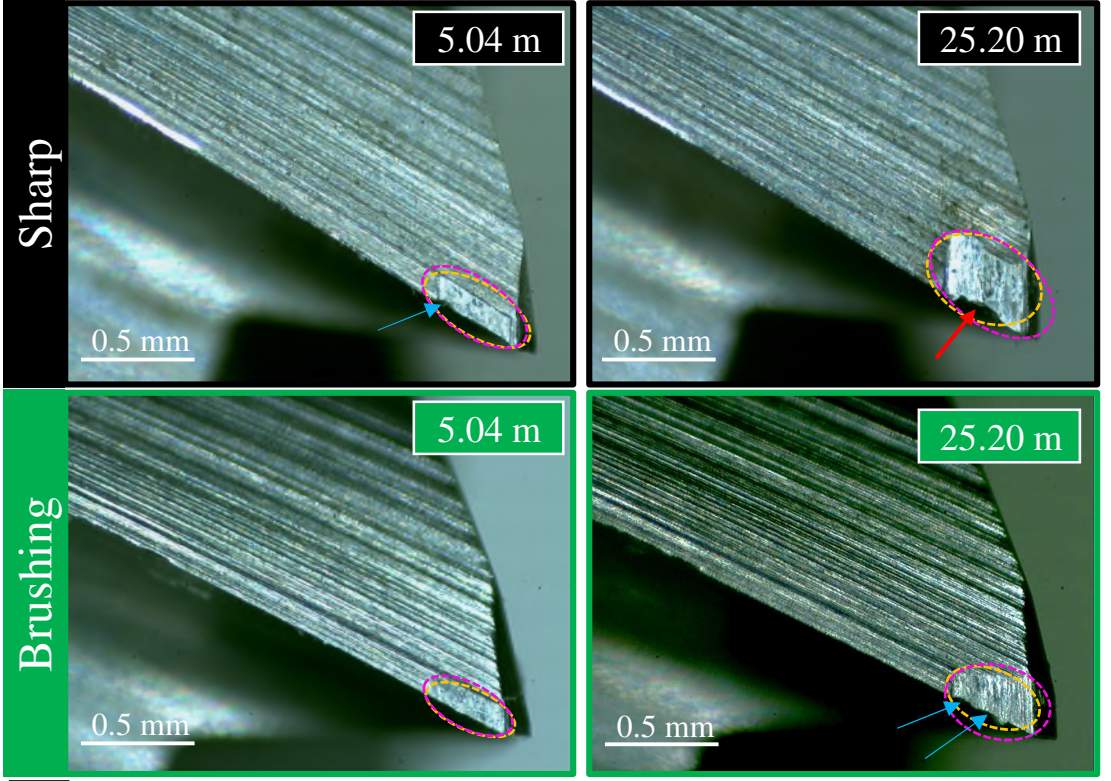
Cutting Tool: WC K40 10% Co End Mill

$\alpha = 10°$	$v_c = 180$ m/min	Dry Cutting
$\gamma = 8°$	$f_z = 0.05$ mm	Down Milling
$\beta = 72°$	$a_p = 0.5$ mm	AISI P20
$\lambda = 30°$	$a_e = 0.2$ mm	37 ± 1 HRC



Brushing Parameters: Config. 15

$v_c = 7.9$ m/s	$a_{pb} = 1$ mm
$v_f = 120$ mm/min	$a_{eb} = 1.5$ mm
$\varphi_b = 15°$	$l_b = 5.3$ mm
t = 60 s	Abrasive: SiC #400



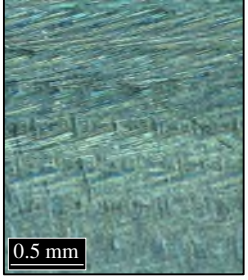
Cutting Tool: WC K40 + 10% Co End Mill

$\alpha = 10^{o}$	$v_c = 180$ m/min	Dry Cutting
$\gamma = 8^{o}$	$f_z = 0.05$ mm	Down Milling
$\beta = 72^{o}$	$a_p = 0.5$ mm	AISI P20
$\lambda = 30^{\circ}$	$a_e = 0.2$ mm	37 ± 1 HRC

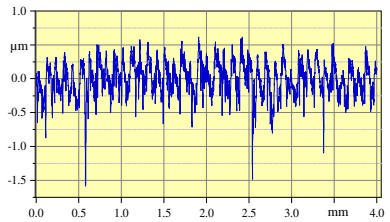


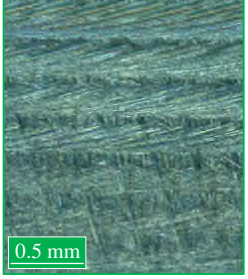
Brushing Parameters: Config. 15

$v_c = 7.9$ m/s	$a_{pb} = 1$ mm
$v_f = 120$ mm/min	$a_{eb} = 1.5$ mm
$\varphi_b = 15^{\circ}$	$l_b = 5.3$ mm
t = 60 s	Abrasive: SiC #400

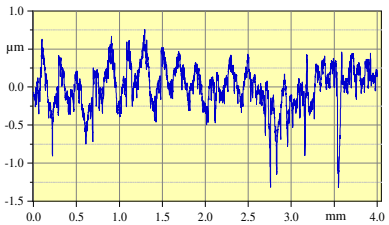


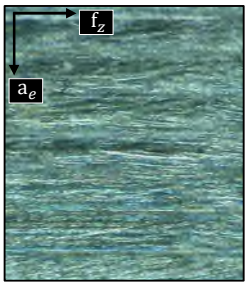
Sharp 0 m





Brushing 0 m





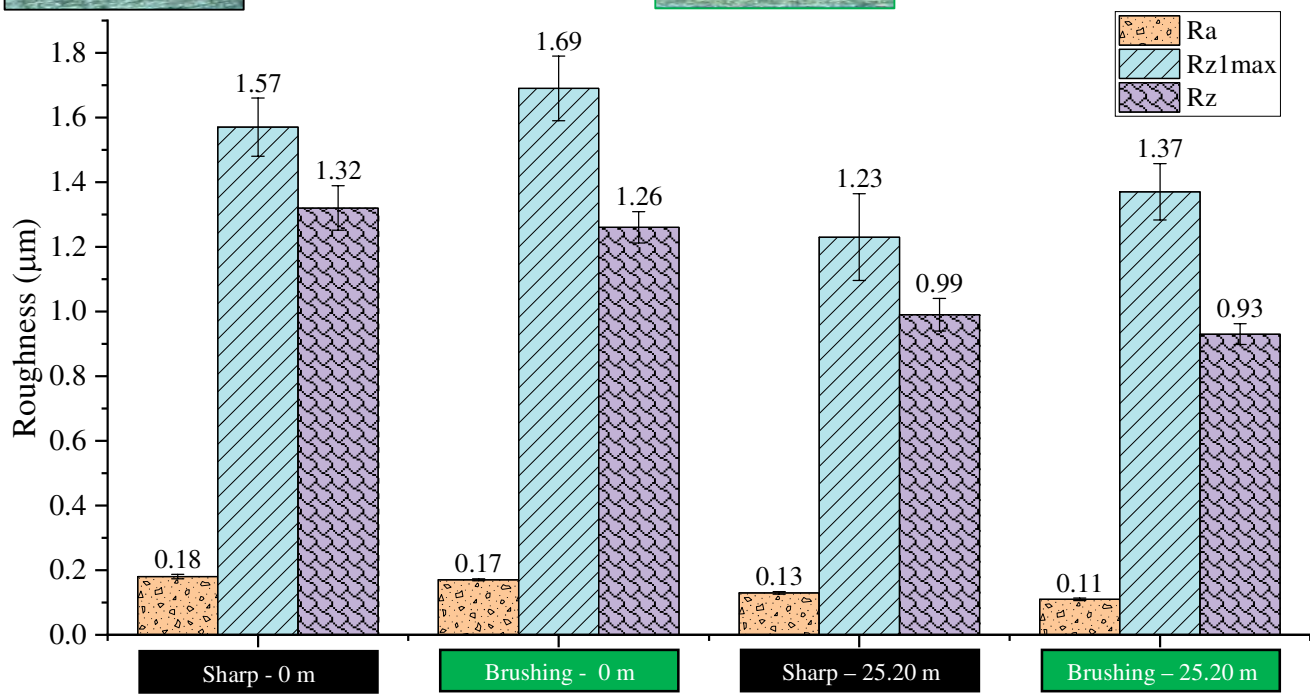
Sharp 25.20 m





Brushing 25.20 m

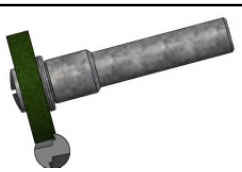




Edge Condition - Cutting Length

Cutting Tool: WC K40 + 10% Co End Mill

$\alpha = 10°$	$v_c = 180$ m/min	Dry Cutting
$\gamma = 8°$	$f_z = 0.05$ mm	Down Milling
$\beta = 72°$	$a_p = 0.5$ mm	AISI P20
$\lambda = 30°$	$a_e = 0.2$ mm	37 ± 1 HRC



Brushing Parameters: Config. 15

$v_c = 7.9$ m/s	$a_{pb} = 1$ mm
$v_f = 120$ mm/min	$a_{eb} = 1.5$ mm
$\varphi_b = 15°$	$l_b = 5.3$ mm
t = 60 s	Abrasive: SiC #400